Safety assessment of chronic oral exposure to iron oxide nanoparticles

Susana Chamorro[1], Lucía Gutiérrez[2], María Pilar Vaquero[1], Dolores Verdoy[3], Gorka Salas[2,4], Yurena Luengo[2], Agustín Brenes[1], and Francisco José Teran[4,5]*

1- Instituto de Ciencia y Tecnología de Alimentos y Nutrición, ICTAN-CSIC, Ciudad Universitaria, José Antonio Novais, 10, 28040 Madrid, Spain

2- Instituto de Ciencia de Materiales de Madrid, ICMM-CSIC, C\Sor Juana Inés de la Cruz, 3, 28049 Madrid, Spain

3- GAIKER-IK4 Technology Centre, Parque Tecnológico, Edificio 202, 48170 Zamudio, Spain

4- IMDEA Nanociencia, Ciudad Universitaria de Cantoblanco, C\Faraday, 9, 28049 Madrid, Spain

5- Unidad Asociada de Nanobiotecnología CNB-CSIC & IMDEA Nanociencia, Campus Universitario de Cantoblanco, 28049 Madrid, Spain

Keywords: nanoparticles, iron oxide, oral exposure, biotransformation, bioavailability, iron absorption

Abstract

Iron oxide nanoparticles with engineered physical and biochemical properties are finding a rapidly increasing number of biomedical applications. However, a wide variety of safety concerns, especially those related to oral exposure, still needs to be addressed in order to reach the clinical practice. Here, we report on the effects of chronic oral exposure to low dose of γ-Fe_2O_3 nanoparticles in growing chickens. Animal observation, weight and diet intake reveal no adverse signs, symptoms, or mortality. No nanoparticle accumulation was observed in liver, spleen and duodenum, while faeces are the main excretion route. Liver iron level and duodenal villi morphology reflect the bioavailability of the iron released from the partial transformation of γ-Fe_2O_3 nanoparticles in acid gastric environment. Duodenal gene expression studies related to the absorption of iron from γ-Fe_2O_3 nanoparticles indicate the enhancement of ferric over ferrous pathway supporting the role of mucins. Our findings

reveal that oral administration of iron oxide nanoparticles is a safe route for drug delivery at low nanoparticle doses.

1. Introduction

Progress in nanotechnology has brought countless novel applications[1] in different areas such as material science, energy or health. In the latest, nanometre-scale chemical engineering is providing novel tools for diagnostics, therapeutics and sensoring[2-3]. One example is given by iron oxide nanoparticles (IONP), which are finding a rapidly increasing number of biomedical applications thanks to their suitable structural, colloidal, and magnetic properties[4]. Nowadays, IONP are employed as suitable platforms for biosensing[2], biomolecular-magnetic trapping[5], magnetic hyperthermia[6], imaging[7], drug- or gene-delivery[8-9]. There is a wide variety of IONP preparation methods providing controllable nanoparticle size and customized physical, chemical and biological functionalities without cytotoxicity drawbacks[4, 10-14]. The coprecipitation of iron salts in water is the most widely used chemical method for synthesis of IONP[14]. Such chemical route provides crystalline IONP from the transformation of a mixture of ferric and ferrous salts in alkaline aqueous medium. Appropriated chemical procedures[4, 15] allow to prepare single-phase IONP avoiding the coexistence of Fe_3O_4 and γ-Fe_2O_3 phases and therefore different iron oxidation states (i.e. Fe(II) and Fe(III)) present into the same nanoparticle.

The success of IONP on distinct biomedical applications requires to overcome safety concerns[16-18]. The assessment of IONP toxicity, biodistribution and excretion routes after long-term exposure is mandatory prior to a safe incorporation into clinical practice. Little attention has been paid to the effects related to IONP oral exposure in spite of the use of engineered nanoparticles for nutritional[19-23] and pharmaceutical [8, 24-25] purposes is expected to increase[20, 26-27]. An important issue is related to the oral administration of nanoparticles where magnetic ones offer the possibility to magnetically guide the drug delivery to intentionally enhance the drug release into the affected tissue[8]. There exist toxicity and gastro-intestinal functioning concerns related to the oral exposure to IONP, especially regarding the absorption of metals like iron[20, 28-29]. Dietary iron is found in two basic forms[30-31], either as haem – found in meat- or non-haem iron -present in cereals, vegetables, beans, fruits, etc. in a number of forms ranging from simple iron oxides and salts to more complex organic chelates. Haem iron is more bioavailable than the non-haem form and their absorption takes place by different pathways. It is well accepted that the main iron absorption takes place in duodenum. In case of non-haem iron, there are two main transport mechanisms to enter into enterocytes. These mechanisms tightly depend on the iron oxidation state: ferrous (i.e. Fe(II)), or ferric (i.e. Fe(III)) forms. Thus, luminal Fe(II) absorption involves divalent metal transporter-1 (DMT1) whereas luminal Fe(III) is proposed to undergo enzymatic reduction to Fe(II), by duodenal cytochrome B (DcytB), prior to apical DMT1 transport from lumen into labile iron pool in the cytoplasm of the enterocytes. Recently, Simovich *et al.* [32] proposed a novel and different ferric pathway at the apical surface of the villus which is specific for the uptake of the ferric form without previous enzymatic reduction. Such iron transport process involves the participation of four proteins in two stages. Firstly, luminal Fe(III) is chelated by mucins, then ferrous iron crosses the membrane in association with β_3-integrin and mobilferrin to internalize into cytosol. Secondly, this Fe(III) and protein complex combines with flavin monooxygenase and β_2-microglobulin (β_2-m) leading to paraferritin complex where Fe(III) is reduced to Fe(II). Once non-haem iron is inside the enterocyte, it can be either stored as ferritin or exported through the basolateral membrane from the ferrous iron pool to blood stream by the combined action of ferroportin (FPN) and hephaestin.[30]

The effects of nanomaterials on intestinal functioning have recently started to be evaluated. Some works on iron containg nanoparticles[20, 23, 33] show that iron from nanoparticles is bioavailable allowing to nanoparticles to act as efficient iron sources spite of the fact the duodenal absorption pathways remain still unknown.[21, 34-35] For this purpose, broiler chicken has been shown to be a suitable and accurate animal model for iron absorption and bioavailability studies[28, 36]. The broiler chickens are useful model for initial screening of Fe bioavailability in foods due to its growth rate, anatomy, size, and low cost. Recent results indicate that this animal model exhibits the appropriate responses to Fe deficiency and has potential to serve as a model for Fe bioavailability[36]. Previous studies related to oral exposure to IONP in mice reveal the genotoxic effects after acute and prolonged oral exposure[16, 25, 37-38]. The controversial variety of results underlines the need to clarify the influence of IONP oral exposure on the intestinal functioning for the sake of safety issues in oral biomedical applications[7-8].

Here, we report on the effects of chronic oral exposure to IONP in growing chickens. Animal observation, diet intake and body weight reveal no adverse signs, symptoms, or mortality after 14 days of low dose IONP oral exposure. No IONP accumulation in liver, spleen and duodenum has been observed, while faeces appear as the main IONP excretion route. In addition, the liver iron level and the duodenal villi morphology reveal that iron from IONP is available. The analysis of haematological parameters indicates normality after chronic IONP dietary treatment. Duodenal gene expression studies on non-haem iron transport indicate that the ferrous pathway is inhibited whilst the ferric pathway is enhanced, supporting the involvement of mucins in iron solubility and transport into enterocytes.

2. Materials and methods

2.1 Synthesis of γ-Fe_2O_3 nanoparticles

The synthesis of γ-Fe_2O_3 nanoparticles coated with amino dextran (AD) was carried out in two steps procedure. In the first step, Fe_3O_4 nanoparticles were synthesized following the co-precipitation protocol described by *Massart et al.*[14] and including some modification[39] of the reaction conditions allows to obtain γ-Fe_2O_3 IONP of 12 nm size and narrow size distribution. In the second step, we proceed to modify the surface of nanoparticles. An aqueous solution of 500 mg of nanoparticles was dispersed in 70 mL of water at pH 11 (adjusted with KOH). AD (500 mg) was dissolved in 30 mL of water and added to nanoparticle dispersion very slowly and sonicated for twelve hours. The excess of coating was washed by dialysis against distilled water. Finally, the particles were dried on a stove to get the γ-Fe_2O_3 IONP powder.

2.2 Structural characterization of γ-Fe_2O_3 nanoparticles

Particle shape, size and size distribution were determined by Transmission Electron Microscopy (TEM) using the 200 KeV JEOL 2000 FXII microscope for routine TEM images and 200 KeV JEOL JEM 2100 for high resolution Transmission Electron Microscopy (HRTEM) images. For that purpose nanoparticles were prepared by placing a drop of a dilute nanoparticle suspension on a carbon-coated copper grid covered with a perforated carbon film and allowing the solvent to evaporate slowly at room temperature. The nanoparticle size is 12 ± 2 nm. The average particle size and distribution were evaluated by measuring the largest internal dimension of 350 particles for the sake of statistical validity. The different size populations are organized into a histogram and are adjusted to a log-normal function. The particle surface coating was characterized by Fourier transform infrared spectra, recorded between 4000 and 300 cm-1 in a Bruker IFS 66 V-S spectrometer. Samples were prepared for infrared characterization by diluting the iron oxide nanoparticle powder in KBr at 2% by weight and compressing the mixture, pressing it into a pellet. On the other hand, quantification of the coating was carried out by simultaneous thermogravimetric analysis and differential thermal analysis performed on a Seiko TG/DTA 320U thermobalance by heating particle dispersion from room temperature to 900 °C at 10 °C/ min under an air flow of 100 ml/ min.

2.3 Magnetic characterization of iron oxide nanoparticles

Magnetization cycles of IONP powder were carried out in a vibrating sample magnetometer 7410 Lakeshore up to 2 T. A mass of 4.6 mg_{Fe} of AD coated IONP powder was introduced into a sample holder for tracing magnetization loops at room temperature while sweeping the magnetic field at 0.25 T/min. Magnetization values are normalized to the γ-Fe_2O_3 mass. In addition, temperature dependence of alternating current (AC) magnetic susceptibility measurements were performed on IONP and mashed freeze-dried liver, spleen and faeces. Samples were transferred into gelatine capsules for AC magnetic susceptibility characterization using a QuantumDesign MPMS-XL SQUID magnetometer. The variation of the AC magnetic susceptibility was recorded under given AC field conditions (11 Hz and 0.41 mT) in a temperature range from 2 to 300 K.

2.4 Diet formulations

Three experimental diets were designed for the experiment. Diet A: basal corn-soybean diet; diet B: basal diet supplemented with ferrous sulphate ($FeSO_4$); diet C: basal diet supplemented with powder of AD coated γ-Fe_2O_3 IONP. Diets in mash form and water were provided ad libitum to birds. All diets were formulated to meet or exceed the minimum requirements established by Spanish Foundation for the Animal Nutrition Development (FEDNA) for broiler chickens[40], except for iron in case of diet A.

2.5 Animal model

A total of 60 one-day-old male broiler chicks (Cobb strain) were housed in electrically heated starter batteries in an environmentally controlled room. From 1st till 7th day, birds were fed ad libitum on diet B with an adaptation period. At the 7th day, 36 birds were selected by similar weight (189 ± 3g) and haemoglobin level. At 8th day, the 36 selected chickens were divided in three groups for receiving different diets during 14 days of dietary treatment period. Each dietary group was allocated in 3 cages (3 replicates with 4 chicks per replicate). At the end of the dietary treatment period (21st day) birds were subjected to 8 hours fasting, and feed consumption per cage was recorded. Then, birds were individually weighted and prepared for blood sample extraction. After blood collection, all chicks were euthanized using carbon dioxide prior to the extraction of duodenal, liver and spleen samples. Experimental procedures were approved by Animal Care and Ethics Committee of Universidad Complutense de Madrid in compliance with the Ministry of Agriculture, Fishery and Food for the Care and Use of Animals for Scientific Purposes.

2.6 Collection of Samples

Faeces: At the 19th day, clean stainless steel collection trays were placed under each cage, for collecting bird excreta during next 48 h (3 replicate per diet, 4 birds per replicate). A subsample of excreta per cage was collected in polyethylene bags and freeze-dried for subsequent determination of iron content. For AC magnetic susceptibility measurements, a pooled sample per diet was prepared out of 3 replicates with 4 birds per replicate. *Blood samples:* 7 birds per diet were randomly selected for blood sample extraction by cardiac puncture. Blood was collected in ethylenediaminetetraacetic acid vacutainer tubes for subsequent determination of haematological parameters. The tubes were centrifuged at 1,500 x g for 10 min, and the supernatants were removed and stored at -20°C until assayed. *Liver and spleen:* samples were washed with saline solution, weighted and frozen at -20º C until lyophilisation. For iron quantification, samples of liver and spleen tissues from 2 birds belonging to same diet were pooled and mashed (6 replicates per diet, 2 birds per replicate). For AC magnetic susceptibility measurements, pooled samples of liver and spleen tissues were prepared from mashed tissues out of 6 replicates with 2 birds per replicate. *Duodenum:* samples from 7 birds per diet were taken and washed with saline solution and divided into 3 different fragments. The first portion of duodenum intestinal mucosa was cleaned with saline solution before preserving in a clean micro-centrifugetube (1.5 ml) and stored at -80ºC after freezing in liquid nitrogen for posterior gene expression study. The second duodenum portion was directly placed in 10% formalin 0.1 phosphate buffer (pH = 7) for subsequent histological studies. The third duodenal portion was frozen at -20ºC until lyophilisation for iron quantification.

2.7 Duodenal morphological studies

Samples were processed for 24 h in a tissue processor with ethanol and were embedded in paraffin. Sections (5 µm) were prepared from duodenal tissue and were stained with hematoxylin-eosin. Histological sections were examined with an an Olimpus optical microscope (Olimpus Optical Co., GmbH, Hamburg,Germany). The images were analyzed using an image software (Soft Imaging System, Olimpus, Hamburg, Germany). The variables measured were villus height, and crypt depth. A total of 10 intact, well-oriented villus-crypt units selected for each intestinal cross-section (6 cross-sections/sample). Villus height (µm) was measured from the tip of the villus to the villus-crypt junction, and crypt depth was defined as the depth of the invagination between adjacent villi. The average of these values was used for statistical analysis.

2.8 Iron quantification in faeces, tissues and diets

Cage pooled faeces, liver, spleen and duodenum tissues were lyophilised and mashed prior to acid digestion. Samples were incubated with 65% nitric acid (1 ml, 1 h, 60°C) for total iron quantification analysis determined per gram of tissue. Quantitative determination of iron was analysed by Inductively Coupled Plasma Atomic Emission Spectroscopy (Perkin Elmer OPTIMA 2100 DV).

2.9 Solubility studies

The solubility tests was done according to the standardized method of *Swain et al.* [41] considering 30 and 60 min as gizzard transit times, 40ºC[42] as physiological temperature and three different pH values (1,2 and 3) to reproduce the acid gastric conditions[43] into gizzard of 21^{st} days old birds. The digestion volume was often gently shaken to simulate the gizzard peristaltic motion. Quantitative determination of iron was analyzed by Inductively Coupled Plasma Atomic Emission Spectroscopy (Perkin Elmer OPTIMA 2100 DV).

2.10 Total RNA Extraction from duodenum tissues

Total RNA was extracted from seven duodenal tissue samples per diet by using RNeasy Mini Kit (Qiagen, Valencia, CA) and following the manufacturer's instruction, (Animal Tissues and Cells, DNase Digest). The extracted RNA mass values ranges from 4 to 29 mg. An automated RNA extraction system (QIAcube system, Qiagen) was used, in order to get the highest reproducibility. Total RNA was finally dissolved in 30 μL elution buffer and stored at –80° C. The quantity and quality of total RNA were assessed on a NanoDrop-ND 1000 (Thermo Fisher Scientific Inc., Boston, MA) and an Agilent 2100 Bioanalyzer, respectively. An aliquot of total RNA (1 μL) was analyzed in an Agilent 2100 Bioanalyzer (Agilent Technologies, Inc., Santa Clara, CA) using appropriated RNA Chips and reagents. The RNA integrity number (RIN) value is an empirical measure of RNA integrity based on the intensities of 28s and 18s rRNA bands. The RIN value is based on an algorithm that assesses a number of features derived from an electropherogram profile for a given sample.

2.11 DMT1, DcytB, FPN and β2-m Gene Expression Analysis

cDNA was produced using the GoTaq Two Step RT-PCR System A6010 (Promega, Madison, WI, USA) in a total volume of 20 µl, with 536 ng of total RNA, following the manufacturer's protocol. No-template and no-reverse-transcription controls were included for each reverse-transcription run for the control treatment. cDNA was stored at -20ºC for later use. Polymerase chain reactions for duodenal DMT1, DcytB and FPN genes were carried out with primers described previously by *Tako et al.*[36], while the β_2-m cDNA was amplified with primers designed by *Yu et al.*[44]. Amplification reactions were performed in a 25 µl volume with 2 µl of cDNA and 250 nM of each primer, in iQ5 96-well PCR plates (Bio-Rad). Thermal cycling conditions consisted of 1 cycle at 95°C for 2 min and 40 cycles of denaturation (15 s) and annealing and extension (60 s). After the reaction, a melting curve analysis from 65ºC to 95ºC was applied to ensure consistency and specificity of the amplified product. Eukaryotic 18S rRNA (Endogenous 18S rRNA, part # 4352930E, Applied Biosystems, Carlsbad, CA, USA) was used as endogenous control for relative gene expression quantification. 18S sRNA was amplified in a different tube. The data mining and quantification of the gene expression levels were determined by the number of cycles needed for the amplification to reach a fixed threshold in the exponential phase of the PCR reaction. The number of cycles is referred to as the quantification cycle (Cq) value. The level of mRNA was normalized to 18S rRNA expression in each sample and presented as the ΔC_q value ($\Delta C_q = C_q$ target mRNA– C_q 18S rRNA)[45]. Real Time PCR analysis of ΔC_q for each sample was performed in triplicate, the average of these three values was used for statistical analysis.

2.12 Statistical analysis

Data from the animal assays were subjected to a one-way analysis of variance by using the general linear model procedure (version 9.2, SAS Institute Inc., Cary, NC). Data are shown as mean values ± standard error of the mean (s.e.m). When the effect was declared significant ($P<0.05$), means were compared using a Tukey's Studentised range test.

3. Results and Discussions

3.1 Iron oxide nanoparticles

Single-phase γ-Fe_2O_3 nanoparticles with AD coating of 12 ± 2 nm size were prepared for dietary Fe(III) supplementation. The as-synthesized are highly crystalline nanostructures as shown in Figure 1. AD coating provides biocompatible features to IONP which have been widely tested in *in vitro* and *in vivo* studies[46]. The magnetic properties of AD coated IONP are shown in Figure 2. On one hand, the magnetization cycles show superparamagnetic features with saturation magnetization values around 70 $A{\cdot}m^2/kg_{\gamma\text{-}Fe2O3}$ and negligible values of remanent magnetization and coercive field at room temperatures. On the other hand, the temperature dependence of the AC magnetic susceptibility is a high-sensitive technique for the detection of IONP in tissues. The AC magnetic susceptibility has two components: the in-phase susceptibility (χ') and the out-of-phase susceptibility (χ''). The out-of-phase component χ''(T) is only sensitive to mineralised iron, as the one forming the AD coated IONP, while the in-phase component χ'(T) includes the contribution from both mineralised iron, paramagnetic iron or other diamagnetic contributions[47]. Figure 2b shows the temperature dependence of χ''of the AD coated IONP powder. Briefly, the temperature behaviour of χ''(T) shows a maximum at around 220 K accompanied by a small shoulder at around 40 K. The maximum observed around 220 K is related to magnetic relaxation processes, while the feature observed at 40 K could be related to an uncoherent reversal of the magnetic moments of single domain non-interacting particles[48]. The overall thermal behaviour of $\chi''(T)$ can be used as an IONP fingerprint for tracking its presence in animal tissues or faeces after 14 days of oral exposure.

3.2 Birds and diets

Growing broiler Cobb chickens were employed in the dietary study. It has been recently shown that broiler chickens are a suitable animal model for iron bioavailability studies due to similarities with the human gastrointestinal tract[28, 36]. The timeline of the experimental procedure, dietary iron dose and sources employed are shown in Figure 3. Initially, 60 male broiler Cobb chickens 1-day-old were fed *ad libitum* with ferrous sulphate supplemented diet (diet B) along an adaptation period of 7 days to warrant an iron sufficient diet avoiding epithelial alteration which may influence the results of our dietary study. After the adaptation period, dietary treatment period starts. From 8th day to 21st day, the bird weight increases 4-fold from 189 ± 3 g to 759 ± 69 g revealing that growing birds need to satisfy strong nutritional requirements along the dietary treatment period. In case of γ-Fe_2O_3 IONP supplemented diet (diet C), the accomplishment of iron requirements implies that each bird would ingest, in average, a total IONP mass of 58 mg along the dietary treatment period.

3.3 Animal observation, food consumption, and body weight

During the period from day 8th to 21st, all birds grew in similar way independently of diet, achieving a similar appearance and average weight (759 ± 69 g) at the end of dietary treatment period. The total fed intake (756 ± 16 g) and weight gain (570 ± 30g) were comparable for all diets along 14 days. In case of birds fed on γ-Fe_2O_3 IONP supplemented diet, the daily IONP dose varies from 24 mg of IONP per kg of bird at day 8th to 6 mg/kg at day 21st when considering the average ingested IONP mass (4 mg) per bird and day and the variation of weight gain along the dietary treatment period, Therefore, the study remains in a low IONP dose range (<300 mg/kg) - according to the dose range established by *Kumari et al.*[37]- where no toxicological effects are expected. Indeed, no adverse signs, symptoms, or mortality were observed in birds fed on γ-Fe_2O_3 IONP supplemented diet. This is reflected on the ratios of fresh liver and spleen/ animal weights, comparable for all diets as shown in Figure 4. The fact that liver and spleen weights are not influenced by diets implies that no toxicological signs such as inflammation were manifested in the animal growth of birds fed on IONP supplemented diet after 14 days.

3.4 IONP biodistribution and excretion

The IONP organ biodistribution analysis after chronic oral exposure was carried out on liver and spleen of birds fed on different diets. Several IONP biodistribution studies in animal models showed preferential accumulation in spleen and liver after intravenous injections, and to a lesser extent in other organs, depending on dosage[49], surface coating[49-50] or intravenous administration methodology[51]. The total IONP intake (58 mg) per bird along the dietary treatment period represents a relevant amount of magnetic nanomaterial for testing their safety since its accumulation in duodenum, spleen and liver can be tracked by AC magnetic measurements. Nonetheless, no signs of IONP accumulation in liver and spleen were observed for birds fed on γ-Fe_2O_3 IONP supplemented diet as shown in Figure 5. These results prove that after IONP oral exposure during 14 days, the accumulated IONP amounts in liver or spleen are insignificant or under the detection limit of AC magnetic susceptibility measurements. IONP do not achieve blood stream from the gastrointestinal tract spite birds were fed *ad libitum* during 14 days. However, faecal AC magnetic data from birds fed on IONP supplemented diet show a $\chi''(T)$ profile (see Figure 5c) which highly resembles the IONP powder data shown in Figure 2b. The slightly different temperature location of the $\chi''(T)$ maximum, in comparison with the IONP powder could be probably related to either a different IONP aggregation degree[49], partial degradation of IONP, or both. In any case, excretion results reveal that IONP are highly ejected along the gastrointestinal tract.

3.5 Influence of dietary IONP treatment on iron storage

The different iron sources employed in diets may result in distinct iron solubility leading to different iron storage and transport pathways. Acid gastric conditions[43] and digestive transit times[42] of twenty-one-days-old Broiler chickens were simulated by *in vitro* acid digestions in order to detect and quantify by analytical means the release of iron atoms from IONP during their degradation. Table 1 shows the results of the iron solubility[52] from IONP under the different pH and acidic digestion times, mimicking gastric digestion conditions. The degradation of γ-Fe_2O_3 nanoparticle releases ferric iron. Solubility values shown in Table 1 are highly low (~2% in the best conditions) for all experimental conditions. These results reflect a poor biodegradation of IONP into Fe(III) under acid gastric conditions, what may explain the large amount of IONP present in faeces observed in Figure 5c. These experiments confirm the intestinal tract as an efficient excretion route. Other relevant information extracted from excreta is that faecal iron level is tightly correlated with diets. The faecal iron level in birds fed on non-iron supplemented diet shows significantly lower value than iron supplemented diets. Since faeces are the main IONP excretion route, we assess their accumulation along intestinal tract by checking the duodenal iron level for different diets. Thus, we observed that duodenal iron level has similar values in birds fed on non-iron and

IONP supplemented diets but these values are significantly lower than for birds fed on ferrous sulphate supplemented diet (see Figure 6d). Such similarities for non-iron and γ-Fe_2O_3 IONP supplemented diets suggest no IONP accumulation in duodenum. The different duodenal iron levels associated with distinct dietary iron sources (i.e. iron sulphate or IONP) can be related to their different iron solubility and/or absorption mechanisms. Indeed, it is well accepted[53] that Fe(II) has higher solubility than Fe(III) leading to higher iron absorption and efflux rates. This is in agreement with the dietary effects on the liver iron shown in Figure 6b for Fe(II) from iron sulphate and Fe(III) from IONP. Liver iron levels are significantly higher in birds fed on ferrous sulphate supplemented diet than in case of non-iron supplemented-one, while IONP supplemented diet shows intermediate values. This is an important result which reflects that iron from IONP is partially bioavailable. Besides, iron amount detected in spleen is similar for all diets (see Figure 6a). Considering that the iron supplement amount ($FeSO_4$ or γ-Fe_2O_3 IONP) represents the 40% of the iron amount present in basal diet (i.e. Diet A), the effects on liver iron underline that iron supplementation by IONP should be considered as physiological.

Haematological parameters have been also analysed since they are expected to be sensitive to iron storage[54]. We have observed no influence of diets on the number of red blood cells, and haematocrit, haemoglobin and serum iron concentrations and their correspondence to bird age (see Tables S1 and S2 in Supporting Information). Similarly, the serum proteinogram does not reflect differences between diets. Hence, haematological data reveal normality after 14 days of oral exposure to IONP as expected for a low dose (i.e. <24 mg/kg)[37].

3.6 Dietary IONP effects on duodenal morphology

Recent works show that the oral exposure to distinct types of nanoparticles may influence the activity of the intestinal epithelium. On one hand, iron- and insulin-containing nanoparticles can be efficiently absorbed acting as efficient iron[55] and insulin sources[24]. On the other hand, chronic and acute oral exposure to polystyrene carboxylated nanoparticles[28] negatively affects iron absorption at the intestinal epithelial layer. In order to assess the expression of any epithelial alteration in birds after 14 days of oral exposure to IONP we have analyzed the morphology of intestinal villi. In general, we observe no alteration or atrophy of duodenal morphology, contrary to recent works[22, 28], which report alterations in the epithelial intestine of chickens after oral exposure to nanoparticles. This can be due to the fact that we use iron sufficient birds avoiding histological changes, which may alter the epithelial functioning. The villi absorption surface tightly depends on the dietary iron as shown in Figure 7 where the villus heights and crypt depths of duodenal tissues are depicted for birds subjected to different diets. While villus height and crypt depth of birds fed on iron supplemented diets are similar, these values are higher than the one observed for the non-iron supplemented diet. Interestingly, these results show that villus morphology is highly related to dietary iron level. This is in agreement with recent results showing that iron deficiency induces gastrointestinal manifestation such as intestinal atrophy whilst non-haematological manifestations are observed[56]. Hence, lower values of villus height and crypt depth are associated with non-iron supplemented diet where dietary iron reduction is around 30% lower than for iron supplemented diets. Furthermore, the intestinal villi development agrees with the liver iron levels shown in Figure 6b. As the IONP accumulation in the liver of birds fed on IONP supplemented diet has not been observed by AC magnetic measurements, we believe that the observed enhancement of liver iron concentration is probably associated with biogenic species such as ferritin. The AC magnetic signal from ferritin is 100 times lower than γ-Fe_2O_3 IONP and its observation requires animals with iron overload [57-58], what is not the case in our study. Thus, the higher villi development observed for birds fed on iron supplemented diets (independently on the iron source) than the non-iron supplemented-one underlines the iron bioavailability from ingested IONP. Recent studies[22-23, 35] show that iron absorption from nanosize structures is favoured in comparison to microsize or bulk courterparts. Furthermore, authors suggest that the luminal non-haem iron released from nanostructures would imply ferrous absorption pathways (i.e. DMT1 and DcytB proteins) without showing experimental evidences.

3.7 Dietary IONP effects on duodenal gene expression

Iron absorption mechanisms are known to depend on iron forms. As mentioned above, it is well accepted the high bioavailability of Fe (II) from iron sulphate[35] and its absorption mechanism involving Dcytb-DMT1 proteins[30]. Figure 8 shows the results of DMT1, DcytB, β_2-m and FPN gene expression analysis. At first glance, the expression of DcytB and DMT1 shows similar values for non-iron supplemented and ferrous sulphate diets but significantly lower than in case of γ-Fe_2O_3 IONP supplemented diet. On the contrary, the β_2-m is significantly overexpressed for birds fed on IONP diet in comparison to control diets. β_2-m which is one of the four proteins involved in the non-haem ferric pathway whose gene expression methodology is available for chickens[44]. Finally, FPN displays similar values for all diets revealing that the iron efflux from enterocyte to blood stream is performed in similar manner independently on the ferrous iron content into the cytoplasm related to different diets. Nevertheless, the downregulation of DMT1 and DcytB genes for γ-Fe_2O_3 IONP supplemented diet suggests an inhibition of ferrous transport pathways while ferric pathway is increased. Such possibility involves mucins, which play an important role to trigger ferric pathways instead of ferrous-ones[32]. This may explain our experimental findings on Fe(III) released from the partial transformation of crystalline γ-Fe_2O_3 nanoparticles under acid gastric conditions. Fe(III) is susceptible to bind mucins[59] favoured by the low solubility of the ferric form into the intestinal mucosa resulting in bioavailable iron.

4. Conclusions

The influence of oral exposure to γ-Fe_2O_3 nanoparticles at low concentration in the diet during 14 days has been assessed in growing broiler chickens. The ingestion of γ-Fe_2O_3 nanoparticles within this growing period has not shown toxicological symptoms on growth parameters, intestinal or haematological alterations. Our results show that γ-Fe_2O_3 nanoparticles are not accumulated in liver, spleen, or duodenum but mainly excreted by faeces. Liver iron level and duodenal villi morphology reveals the bioavailability of Fe(III) resulting from a partial transformation of γ-Fe_2O_3 nanoparticles under acid gastric environment. Iron absorption mechanisms are assessed after oral exposure to iron containing nanoparticles. Duodenal gene expression studies related to non-haem iron proteins indicates that ferrous pathways are inhibited while ferric pathways are enhanced suggesting the participation of mucins in the iron transport into enterocytes. Our findings reveal that oral administration of iron oxide nanoparticles is a safe route for drug delivery at low dose. Nanotechnology opens new avenues towards nanoparticle engineering for providing customized iron forms and fractions, allowing to control iron solubility and absorption rates.

Acknowledgements

This work has been partially supported by European Commission (MULTIFUN, nº 262943), Spanish Ministry of Economy and Competitiveness (MAT2010-21822-C02-01). F.J.T acknowledges financial support from Ramon y Cajal subprogram (RYC-

2011-09617) and L.G. is the beneficiary of a post-doctoral grant from the AXA Research Fund. We thank Dr. Agustín Viveros and Dr. María Luisa Fermín for haematological analysis, and Dr. María del Puerto Morales for her interest in this work and fruitful discussions. Dr. Alberto Bollero, Karol Golasiński and Servicio General de Apoyo a la Investigación de la Universidad de Zaragoza are acknowledged for magnetic measurements.

Figures and Tables

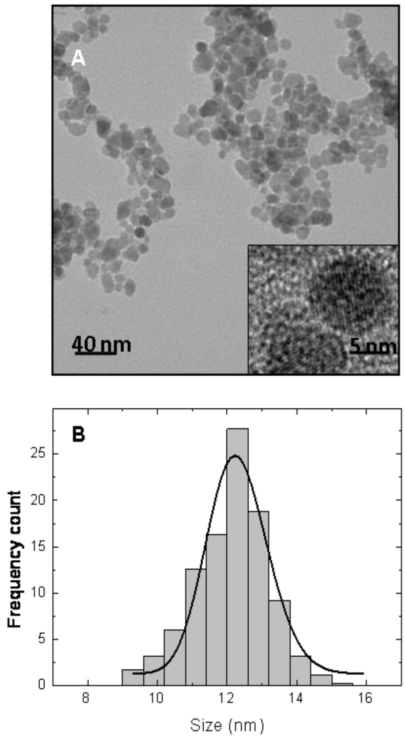

Figure 1. Structural characterization of nanoparticles (A) TEM micrograph of IONP. Scale bar:40 nm. Inset: HRTEM micrograph of IONP. Scale bar: 5 nm, (B) size distribution (log normal fit) of IONP.

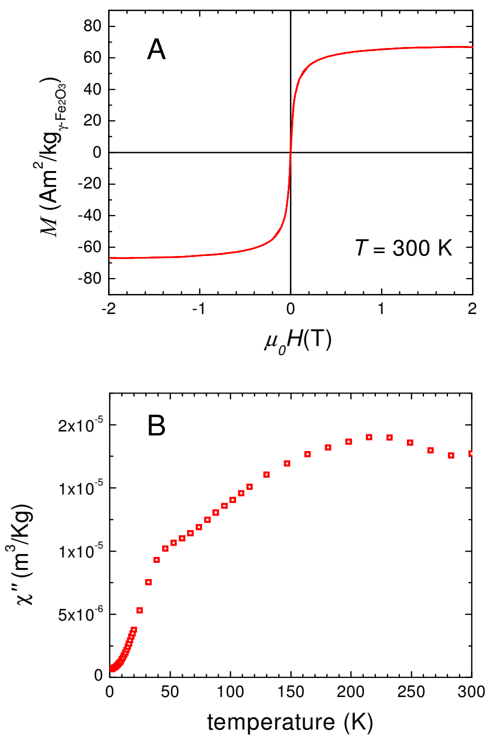

Figure 2. Magnetic characterization of nanoparticles (A) Mass-normalized magnetization cycle of IONP powder at room temperature, (B) Temperature dependence of χ'' of IONP powder.

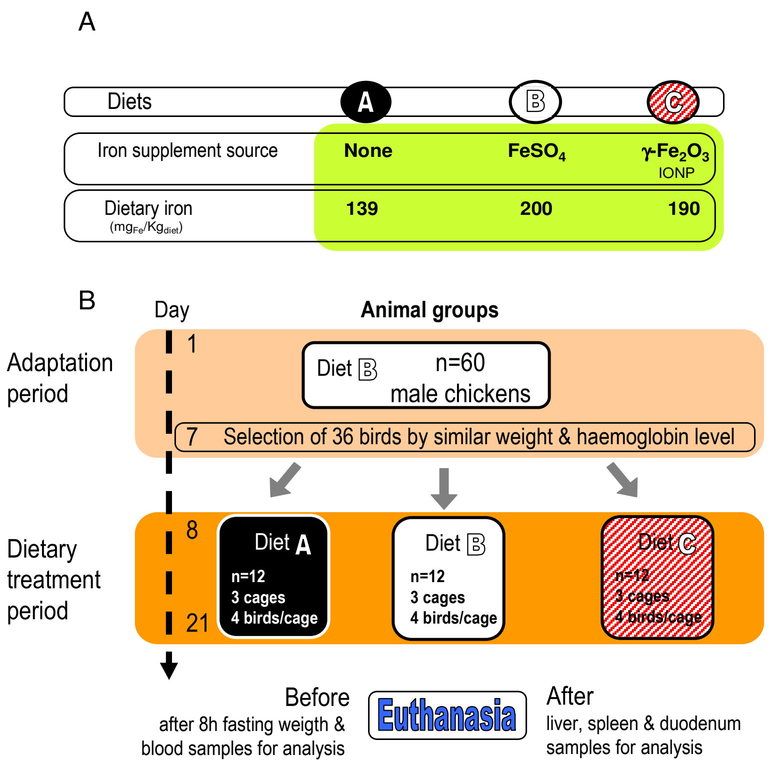

Figure 3. Timeline and experimental design (A) Dietary iron source and dose, (B) Timeline of animal feeding and selection schedule, animal groups, diets, selection criteria, and sample collection.

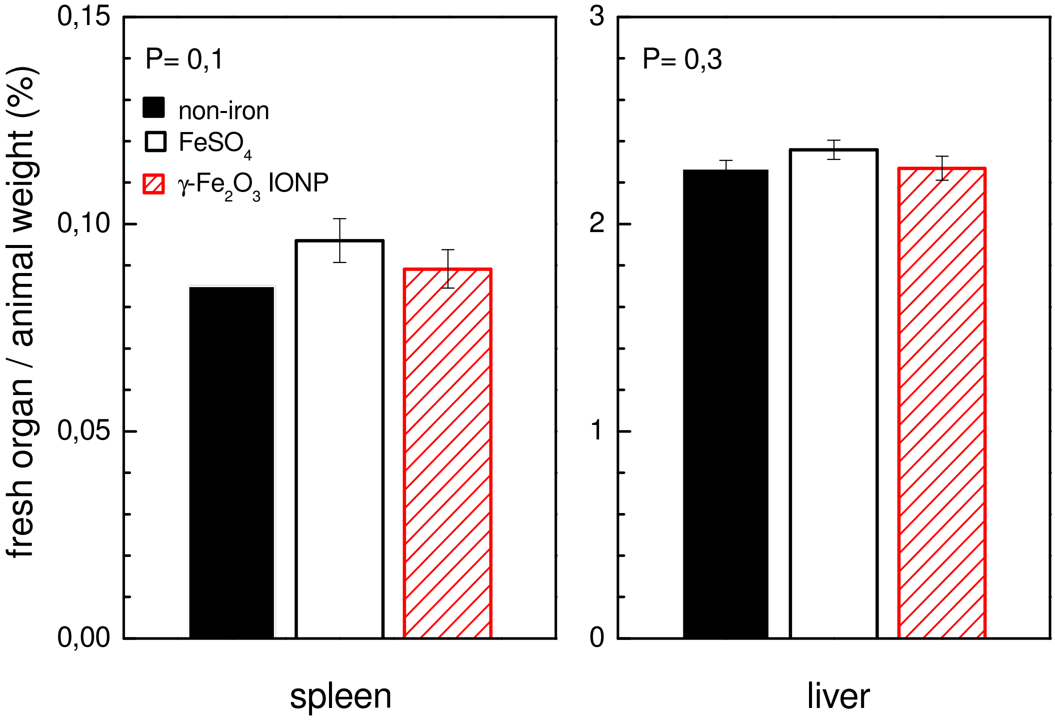

Figure 4. Influence of diets on fresh organ weight (A) fresh spleen/animal weight ratio (n=12), (B) fresh liver/animal weight ratio (n=12). Error bars, ± s.em.

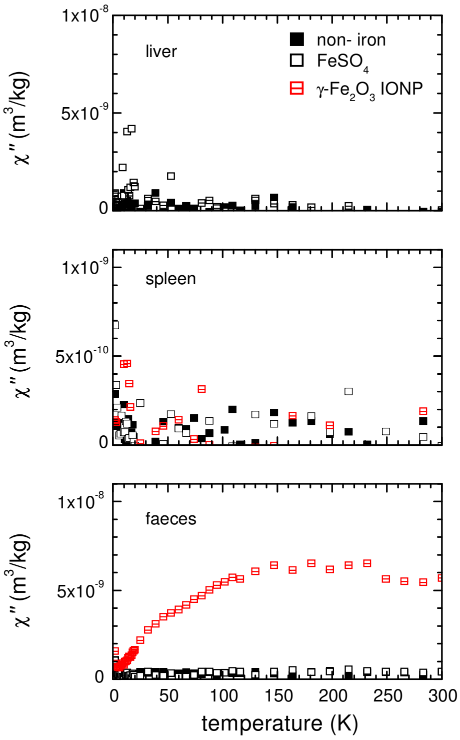

Figure 5. Temperature dependence of χ” in different tissues from birds fed on different diets (A) liver tissues, (B) spleen tissues, (C) faeces. In (A,B), pooled samples of liver and spleen tissues were prepared from mashed tissues out of 6 replicates with 2 birds per replicate. In (C), pooled sample per diet was prepared out of 3 replicates with 4 birds per replicate.

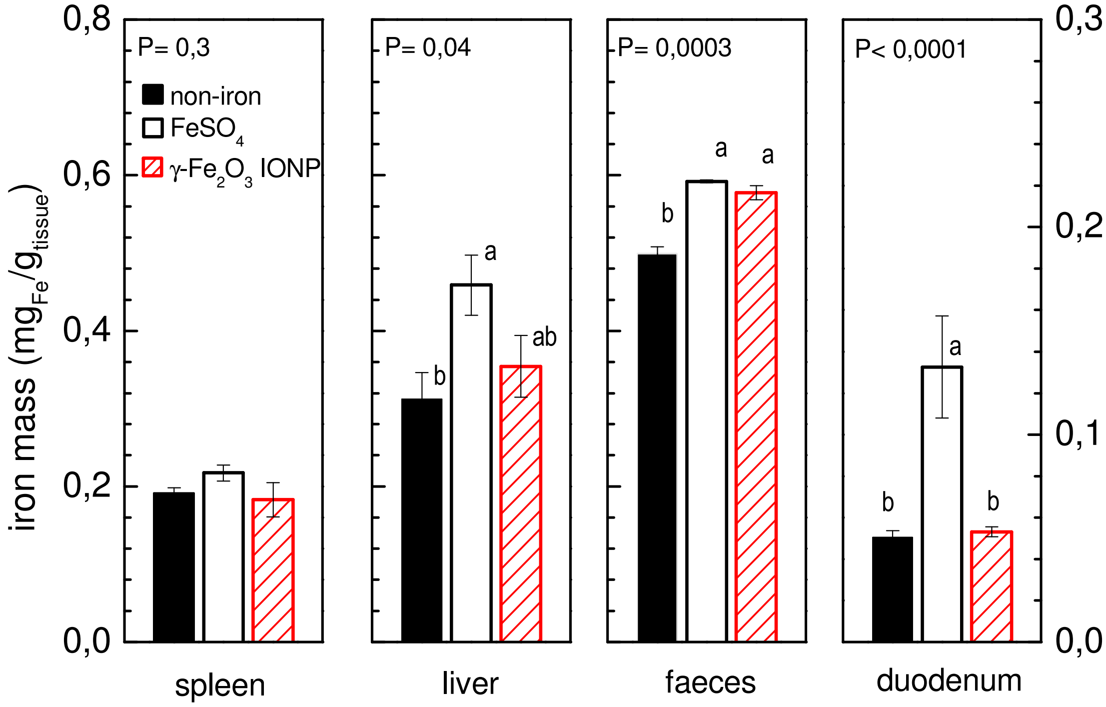

Figure 6. Influence of diets on the iron concentration in (A) spleen tissues (n=6 replicates,2 birds/replicate), (B) liver tissues (n=6 replicates,2 birds/replicate), (C) pen pooled faeces (n=3 replicates,4 birds/replicate), (D) duodenum tissues (n=7). Error bars, ± s.e.m. In (B-D), significant dietary differences ($P<0.05$) on iron liver, spleen and duodenum average concentration values are indicated by contrast characters (a,b) according to a one way analysis of variance with Tukey's post test.

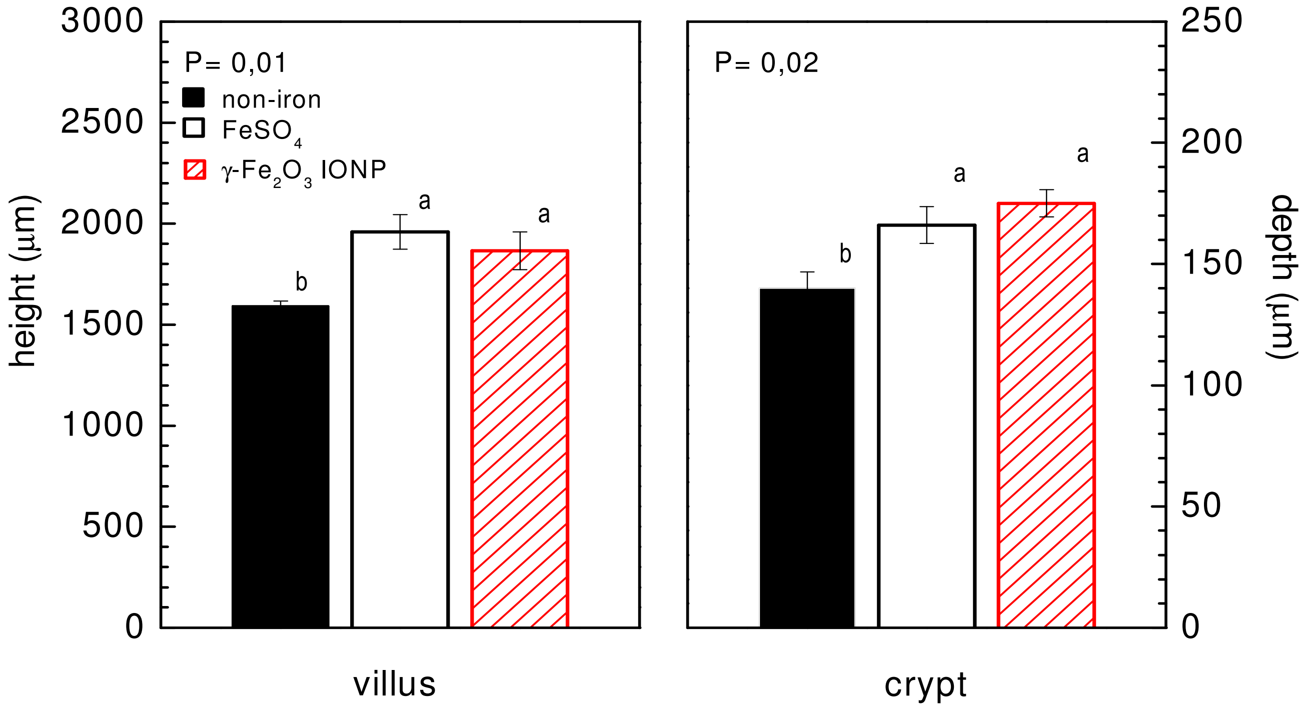

Figure 7: Influence of diets on duodenal morphological parameters (A) villus height (n=7), (B) crypt depth (n=7). Error bars, ± s.e.m. In (A-B), significant dietary differences ($P<0.05$) on average villus and crypth values are indicated by contrast characters (a,b) according to a one way analysis of variance with Tukey's post test.

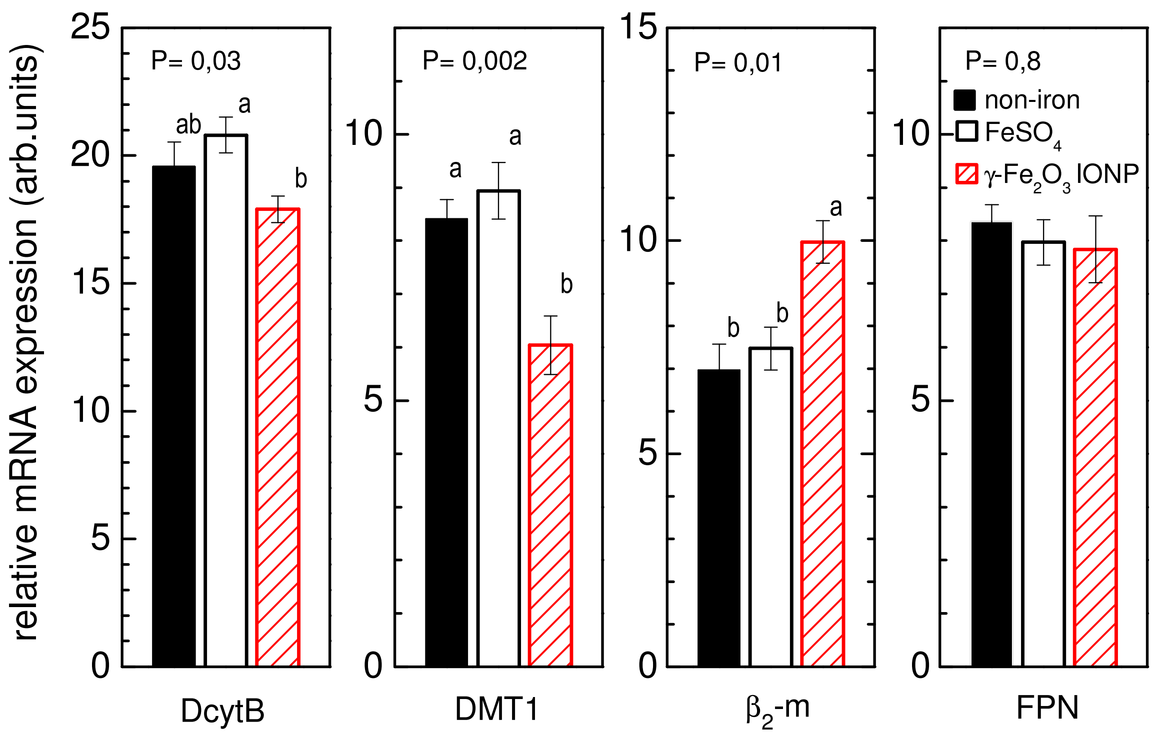

Figure 8. Influence of diets on mRNA expression of duodenal genes (A) DcytB, (B) DMT1,(C) β2-m, (D) FPN. Gene expression levels were determined by real-time quantitative reverse-transcription-polymerase chain reaction (n = 7) and expressed relative to 18S rRNA in arbitrary units (a.u.).Error bars, ± s.e.m. In (A-C), significant dietary differences ($P<0.05$) on mRNA expression are indicated by contrast characters (a,b) according to a one way analysis of variance with Tukey's post test.

Table 1. Solubility of Fe from IONP under different pH and digestion times, mimicking gastric digestion conditions.

pH	Digestion Time (min)	Total Fe mass (μg)	Released Fe mass (μg)	Fe solubility (%)
1	30	2770	43	1.6
1	60	3020	57	1.9
2	30	2560	9	0.3
2	60	2920	12	0.4
3	30	2550	4	0.2
3	60	2870	5	0.2

References

[1] Directorate of Research & Innovation E C 2011 Nanotechnology applications

[2] Haun J B, Yoon T-J, Lee H and Weissleder R 2010 Magnetic nanoparticle biosensors *Wiley Interdisciplinary Reviews: Nanomedicine and Nanobiotechnology* 2 291-304

[3] Hilger I and Kaiser W A 2012 Iron oxide-based nanostructures for MRI and magnetic hyperthermia *Nanomedicine* 7 1443-59

[4] Costo R, Bello V, Robic C, Port M, Marco J F, Puerto Morales M and Veintemillas-Verdaguer S 2012 Ultrasmall Iron Oxide Nanoparticles for Biomedical Applications: Improving the Colloidal and Magnetic Properties *Langmuir* 28 178-85

[5] Konry T, Bale S, Bhushan A, Shen K, Seker E, Polyak B and Yarmush M 2012 Particles and microfluidics merged: perspectives of highly sensitive diagnostic detection *Microchimica Acta* 176 251-69

[6] Maier-Hauff K, Ulrich F, Nestler D, Niehoff H, Wust P, Thiesen B, Orawa H, Budach V and Jordan A 2011 Efficacy and safety of intratumoral thermotherapy using magnetic iron-oxide nanoparticles combined with external beam radiotherapy on patients with recurrent glioblastoma multiforme *J. Neurooncol.* 103 317-24

[7] Hahn P, Stark D, Lewis J, Saini S, Elizondo G, Weissleder R, Fretz C and Ferrucci J 1990 First clinical trial of a new superparamagnetic iron oxide for use as an oral gastrointestinal contrast agent in MR imaging. *Radiology* 175 6

[8] Seth A, Lafargue D, Poirier C, Péan J-M and Ménager C Performance of magnetic chitosan–alginate core–shell beads for increasing the bioavailability of a low permeable drug *Eur. J. Pharm. Biopharm.*

[9] Dobson J 2006 Gene therapy progress and prospects: magnetic nanoparticle-based gene delivery *Gene Ther.* 13 283-7

[10] Roca A G, Costo R, Rebolledo A F, Veintemillas-Verdaguer S, Tartaj P, González-Carreño T, Morales M P and Serna C J 2009 Progress in the preparation of magnetic nanoparticles for applications in biomedicine *J. Phys. D: Appl. Phys.* 42 224002

[11] Prina-Mello A, Crosbie-Staunton K, Salas G, del Puerto Morales M and Volkov Y 2013 Multiparametric Toxicity Evaluation of SPIONs by High Content Screening Technique: Identification of Biocompatible Multifunctional Nanoparticles for Nanomedicine *Magnetics, IEEE Transactions on* 49 377-82

[12] Mejías R, Gutiérrez L, Salas G, Pérez-Yagüe S, Zotes T M, Lázaro F J, Morales M P and Barber D F 2013 Long term biotransformation and toxicity of dimercaptosuccinic acid-coated magnetic nanoparticles support their use in biomedical applications *J. Controlled Release* 171 225-33

[13] Luengo Y, Nardecchia S, Morales M P and Serrano M C 2013 Different cell responses induced by exposure to maghemite nanoparticles *Nanoscale* 5 11428-37

[14] Massart R 1981 Preparation of aqueous magnetic liquids in alkaline and acidic media *Magnetics, IEEE Transactions on* 17 1247-8

[15] Morales M P, Veintemillas-Verdaguer S, Montero M I, Serna C J, Roig A, Casas L, Martínez B and Sandiumenge F 1999 Surface and Internal Spin Canting in γ-Fe2O3 Nanoparticles *Chem. Mater.* 11 3058-64

[16] Singh N, Manshian B, Jenkins G J S, Griffiths S M, Williams P M, Maffeis T G G, Wright C J and Doak S H 2009 NanoGenotoxicology: The DNA damaging potential of engineered nanomaterials *Biomaterials* 30 3891-914

[17] Foy S P and Labhasetwar V 2011 Oh the irony: Iron as a cancer cause or cure? *Biomaterials* 32 9155-8

[18] Gu L, Fang R H, Sailor M J and Park J-H 2012 In Vivo Clearance and Toxicity of Monodisperse Iron Oxide Nanocrystals *ACS Nano* 6 4947-54

[19] Miller D D 2010 Food nanotechnology: New leverage against iron deficiency *Nat Nano* 5 318-9

[20] Pereira D I A, Bruggraber S F A, Faria N, Poots L K, Tagmount M A, Aslam M F, Frazer D M, Vulpe C D, Anderson G J and Powell J J 2014 Nanoparticulate iron(III) oxo-hydroxide delivers safe iron that is well absorbed and utilised in humans *Nanomed. Nanotechnol. Biol. Med.*

[21] Aslam M F, Frazer D M, Faria N, Bruggraber S F A, Wilkins S J, Mirciov C, Powell J J, Anderson G J and Pereira D I A 2014 Ferroportin mediates the intestinal absorption of iron from a nanoparticulate ferritin core mimetic in mice *The FASEB Journal* 28 3671-8

[22] Hilty F M, Arnold M, Hilbe M, Teleki A, Knijnenburg J T N, Ehrensperger F, Hurrell R F, Pratsinis S E, Langhans W and Zimmermann M B 2010 Iron from nanocompounds containing iron and zinc is highly bioavailable in rats without tissue accumulation *Nat Nano* 5 374-80

[23] Hilty F M, Teleki A, Krumeich F, Büchel R, Hurrell R F, Pratsinis S E and Zimmermann M B 2009 Development and optimization of iron- and zinc-containing nanostructured powders for nutritional applications *Nanotechnology* 20 475101

[24] Lopes M A, Abrahim B A, Cabral L M, Rodrigues C R, Seiça R M F, de Baptista Veiga F J and Ribeiro A J 2014 Intestinal absorption of insulin nanoparticles: Contribution of M cells *Nanomed. Nanotechnol. Biol. Med.* 10 1139-51

[25] Fu C, Liu T, Li L, Liu H, Chen D and Tang F 2013 The absorption, distribution, excretion and toxicity of mesoporous silica nanoparticles in mice following different exposure routes *Biomaterials* 34 2565-75

[26] Sozer N and Kokini J L 2009 Nanotechnology and its applications in the food sector *Trends Biotechnol.* 27 82-9

[27] Timko B P, Whitehead K, Gao W, Kohane D S, Farokhzad O, Anderson D and Langer R 2011 Advances in Drug Delivery *Annual Review of Materials Research* 41 1-20

[28] Mahler G J, Esch M B, Tako E, Southard T L, Archer S D, Glahn R P and Shuler M L 2012 Oral exposure to polystyrene nanoparticles affects iron absorption *Nat Nano* 7 264-71

[29] Powell J J, Faria N, Thomas-McKay E and Pele L C 2010 Origin and fate of dietary nanoparticles and microparticles in the gastrointestinal tract *J. Autoimmun.* 34 J226-J33

[30] Sharp P and Srai S K 2007 Molecular mechanisms involved in intestinal iron absorption *World Journal of Gastroenterology* 13 9

[31] West A R and Oates P S 2008 Mechanisms of heme iron absorption: Current questions and controversies *World Journal of Gastroenterology* 14 4101-10

[32] Simovich M, Hainsworth L N, Fields P A, Umbreit J N and Conrad M E 2003 Localization of the iron transport proteins mobilferrin and DMT-1 in the duodenum: The surprising role of mucin *Am. J. Hematol.* 74 32-45

[33] Gastearena M A I, Gil A G, Azqueta A, Coronel M P and Gimeno M 2003 A comparative study on the gastroduodenal tolerance of different antianaemic preparations *Hum. Exp. Toxicol.* 22 137-41

[34] Pereira D I A, Mergler B I, Faria N, Bruggraber S F A, Aslam M F, Poots L K, Prassmayer L, Lönnerdal B, Brown A P and Powell J J 2013 Caco-2 Cell Acquisition of Dietary Iron(III) Invokes a Nanoparticulate Endocytic Pathway *PLoS ONE* 8 e81250

[35] Zimmermann M B and Hilty F M 2011 Nanocompounds of iron and zinc: their potential in nutrition *Nanoscale* 3 2390-8

[36] Tako E, Rutzke M A and Glahn R P 2010 Using the domestic chicken (Gallus gallus) as an in vivo model for iron bioavailability *Poult. Sci.* 89 514-21

[37] Kumari M, Rajak S, Singh S P, Murty U S N, Mahboob M, Grover P and Rahman M F 2013 Biochemical alterations induced by acute oral doses of iron oxide nanoparticles in Wistar rats *Drug Chem. Toxicol.* 36 296-305

[38] Singh S P, Rahman M F, Murty U S N, Mahboob M and Grover P 2013 Comparative study of genotoxicity and tissue distribution of nano and micron sized iron oxide in rats after acute oral treatment *Toxicol. Appl. Pharmacol.* 266 56-66

[39] de la Presa P, Luengo Y, Multigner M, Costo R, Morales M P, Rivero G and Hernando A 2012 Study of Heating Efficiency as a Function of Concentration, Size, and Applied Field in γ-Fe2O3 Nanoparticles *The Journal of Physical Chemistry C* 116 25602-10

[40] de Blas C, Mateos G G and García-Rebollar P 2010 Tablas FEDNA de composición y valor nutritivo de alimentos para la fabricación de piensos compuestos *Fundación Española para el Desarrollo de la Nutrición Animal, Madrid* 502

[41] Swain J H, Newman S M and Hunt J R 2003 Bioavailability of Elemental Iron Powders to Rats Is Less than Bakery-Grade Ferrous Sulfate and Predicted by Iron Solubility and Particle Surface Area *The Journal of Nutrition* 133 3546-52

[42] Rougière N and Carré B 2010 Comparison of gastrointestinal transit times between chickens from D+ and D− genetic lines selected for divergent digestion efficiency *animal* 4 1861-72

[43] Herpol C and Van Grembergen G 1967 La signification du pH dans le tube digestif de gallus domesticus *Ann. Biol. Anim. Biochim. Biophys.* 7 33–8

[44] Yu C, Liu Q, Qin A, Hu X, Xu W, Qian K, Shao H and Jin W 2013 Expression kinetics of chicken β2-microglobulin and Class I MHC in vitro and in vivo during Marek's disease viral infections *Vet. Res. Commun.* 37 277-83

[45] Livak K J and Schmittgen T D 2001 Analysis of Relative Gene Expression Data Using Real-Time Quantitative PCR and the 2−ΔΔCT Method *Methods* 25 402-8

[46] Simberg D, Park J-H, Karmali P P, Zhang W-M, Merkulov S, McCrae K, Bhatia S N, Sailor M and Ruoslahti E 2009 Differential proteomics analysis of the

surface heterogeneity of dextran iron oxide nanoparticles and the implications for their in vivo clearance *Biomaterials* 30 3926-33

[47] Gutierrez L, Morales M P and Lazaro F J 2014 Prospects for magnetic nanoparticles in systemic administration: synthesis and quantitative detection *PCCP* 16 4456-64

[48] Lázaro F J, Larrea A and Abadı́a A R 2003 Magnetostructural study of iron–dextran *J. Magn. Magn. Mater.* 257 346-54

[49] Gutiérrez L, Mejías R, Barber D F, Veintemillas-Verdaguer S, Serna C J, Lázaro F J and Morales M P 2011 Ac magnetic susceptibility study of in vivo nanoparticle biodistribution *J. Phys. D: Appl. Phys.* 44 255002

[50] Cole A J, David A E, Wang J, Galbán C J and Yang V C 2011 Magnetic brain tumor targeting and biodistribution of long-circulating PEG-modified, cross-linked starch-coated iron oxide nanoparticles *Biomaterials* 32 6291-301

[51] Gutierrez L, Mejias R, Lazaro F J, Serna C J, Barber D F and Morales M P 2013 Effect of Anesthesia on Magnetic Nanoparticle Biodistribution After Intravenous Injection *Magnetics, IEEE Transactions on* 49 398-401

[52] Fe solubility = 100 x Released Fe / Total Fe

[53] Whitehead M W, Thompson R P and Powell J J 1996 Regulation of metal absorption in the gastrointestinal tract. *Gut* 39 625-8

[54] Mitchell T R, Anderson D and Shepperd J 1980 IRON DEFICIENCY, HÆMOCHROMATOSIS, AND GLYCOSYLATED HÆMOGLOBIN *The Lancet* 316 747

[55] Powell J J, Bruggraber S F A, Faria N, Poots L K, Hondow N, Pennycook T J, Latunde-Dada G O, Simpson R J, Brown A P and Pereira D I A 2014 A nano-disperse ferritin-core mimetic that efficiently corrects anemia without luminal iron redox activity *Nanomed. Nanotechnol. Biol. Med.* 10 1529-38

[56] Lizarraga A, Cuerda C, Junca E, Bretón I, Camblor M, Velasco C and García-Peris P 2009 Atrophy of the intestinal villi in a post-gastrectomy patient with severe iron deficiency anemia *Nutr. Hosp.* 24 618-21

[57] Gutiérrez L, Quintana C, Patiño C, Bueno J, Coppin H, Roth M P and Lázaro F J 2009 Iron speciation study in Hfe knockout mice tissues: Magnetic and ultrastructural characterisation *Biochimica et Biophysica Acta (BBA) - Molecular Basis of Disease* 1792 541-7

[58] Gutiérrez L, Vujić Spasić M, Muckenthaler M U and Lázaro F J 2012 Quantitative magnetic analysis reveals ferritin-like iron as the most predominant iron-containing species in the murine Hfe-haemochromatosis *Biochimica et Biophysica Acta (BBA) - Molecular Basis of Disease* 1822 1147-53

[59] Conrad M E and Umbreit J N 1993 A concise review: Iron absorption—The mucin-mobilferrin-integrin pathway. A competitive pathway for metal absorption *Am. J. Hematol.* 42 67-73